

# The effect of noise and sampling size on vorticity measurements in rotating fluids

Kelvin K.L. Wong<sup>a</sup>, Richard M. Kelso<sup>b</sup>, Jagannath Mazumdar<sup>a</sup> and Derek Abbott<sup>a</sup>

<sup>a</sup>Center for Biomedical Engineering and School of Electrical & Electronics Engineering,  
University of Adelaide, SA 5005, Australia;

<sup>b</sup>School of Mechanical Engineering, University of Adelaide, SA 5005, Australia

## ABSTRACT

This paper describes a new technique for presenting information based on given flow images. Using a multi-step first order differentiation technique, we are able to map in two dimensions, vorticity of fluid within a region of investigation. We can then present the distribution of this property in space by means of a color intensity map. In particular, the state of fluid rotation can be displayed using maps of vorticity flow values. The framework that is implemented can also be used to quantify the vortices using statistical properties which can be derived from such vorticity flow maps. To test our methodology, we have devised artificial vortical flow fields using an analytical formulation of a single vortex. Reliability of vorticity measurement from our results shows that the size of flow vector sampling and noise in flow field affect the generation of vorticity maps. Based on histograms of these maps, we are able to establish an optimised configuration that computes vorticity fields to approximate the ideal vortex statistically. The novel concept outlined in this study can be used to reduce fluctuations of noise in a vorticity calculation based on imperfect flow information without excessive loss of its features, and thereby improves the effectiveness of flow

**Keywords:** Vorticity, Flow visualisation, Reliability, Histogram, Oseen vortex

## 1. INTRODUCTION

Flow visualisation is the technique of examining fluid flow and to be able to interpret its structure and obtain qualitative information about other flow parameters within the flow field. Two dimensional flow imaging such as particle image velocimetry,<sup>1,2</sup> phase contrast magnetic resonance velocimetry<sup>3</sup> or fluid motion estimating<sup>4</sup> have been used to generate vector fields of the fluid flow. However, imperfect measurement conditions and equipment noise fluctuations often render the flow measurement non-ideal and generate a certain percentage of error in measurement.

In many instances, post processing of flow data such as replacement of inaccurate vectors using the median test<sup>2</sup> followed by outlier replacement to synthesise filtered vectors can be deployed to improve flow mapping accuracy. Derivative estimation from the flow based on the processed data is typically performed for a more concise flow analysis. Despite efforts to clean up noise in the data and to improve accuracy of this derivative estimation,<sup>5-8</sup> vorticity analysis will often be biased due to the presence of noise in the flow field. This is because the visualisation of fluid rotation using vorticity mapping will be affected by the uncertainty of field vector misalignments which distorts the vorticity values computed. In addition, use of only a single contour of vectors at each digitised flow field map frame of interrogation for the vorticity computation gives a poor representation of the overall vorticity map in the event of high incidence of noise in the flow information.

---

Further author information: (Send correspondence to K.K.L. Wong)

K.K.L. Wong: E-mail: kwong@eleceng.adelaide.edu.au, Telephone: +61 (8) 8303 6296

R.M. Kelso: E-mail: rmkelso@mecheng.adelaide.edu.au, Telephone: +61 (8) 8303 5460, Fax: +61 (8) 8303 4367

J. Mazumdar: E-mail: jagan.mazumdar@adelaide.edu.au, Telephone: +61 (8) 8303 5084

D. Abbott: E-mail: dabbott@eleceng.adelaide.edu.au, Telephone: +61 (8) 8303 5748, Fax: +61 (8) 8303 4360

From estimating graph gradients numerically, we can develop a set of equations that explain how to derive flow derivatives based on multiple layers of vector contours around a region of interrogation. Using more than one layer of contours which are encapsulated by a larger sampling window size, we intrinsically averaged a larger group of the flow data while providing an indication of the fluid vorticity at a point of interest. However, the sampling window configuration of the calculation needs to be selected optimally to produce vorticity maps that relate to that of an analytically correct vortex to the maximum extent. Over sizing the window destroy the critical flow features while undersizing it gives a poor global representation of the vorticity map of a vortex. It is therefore of interest to develop a framework for analysing the reliability of vorticity sampling and calculation to best represent vortical flow mapping and visualisation. To solve the problem, we developed a framework that can test the reliability of the computation based on a specific sampling window configuration. It is worthwhile noting that this reliability study has its basis on the statistics of vorticity distribution pertaining to the flow derivative map.

This paper is structured as follows. A background on the Oseen vortex formulation is provided since the synthetic flow fields used in our experiments is constructed using the velocity profiles described by the analytical equations. The theoretical outline of our vorticity quantification is given. Next, experimental techniques for vector field generation are described. The results and discussion section analyses the statistical behaviour of vorticity fields and conceptualises the framework for optimisation of vorticity visualisation. Finally, a summary of the implemented methodology and vorticity visualisation results is given in conclusion.

## 2. THEORY

### 2.1 Analytical Formulation of Vortex

The Oseen vortex is a model of a real vortex with analytically defined velocity, vorticity and circulation.<sup>9-11</sup> The angular velocity  $\omega(r)$  is described in Equation 1. We set the tangential velocity  $V_\theta(r)$  as a function of  $r$  in Equation 2. If  $\Gamma_0$  is the circulation, and  $L$  is the length scale corresponding to one standard deviation of the Gaussian vorticity distribution of the vortex, we have

$$\omega(r) = \frac{\Gamma_0}{2\pi L^2} \left( e^{-\frac{r^2}{2L^2}} \right) \quad (1)$$

$$V_\theta(r) = \frac{\Gamma_0}{2\pi r} \left( 1 - e^{-\frac{r^2}{2L^2}} \right) \quad (2)$$

We can digitise the analytic velocity field over an image grid with each coordinate denoted by  $(x, y)$ , and with velocity interrogation spacing,  $\delta$  to produce a velocity vector flow field,  $u_{x,y}$  at a resolution of  $\frac{\delta}{L}$ . This allows the effect of velocity field resolution based on the analytical data produced for our computational approach to be quantified. Note that the tangential velocity at the core is zero despite having a finite vorticity.

### 2.2 Vorticity Measurement and Statistics of Flow Map

A definition of vorticity is provided by examining the magnitude of rotation of fluid about a specific examined point. This may be demonstrated by schematic elements in Figure 1(a). For numerical derivation of circulation, the summation of velocity vectors multiplied by the finite interval distance in the same direction and in the counter-clockwise direction around this point of measurement is performed. The vorticity  $\omega$  is obtained by dividing the local circulation with the sampling or interrogation window that is the finite quantification of the area swept by this rotational flow. The vorticity is represented by a normal component of the in-plane flow which passes through the plane.

Note that in order to evaluate such integrals, an appropriate path or region of integration is to be chosen appropriately. Studies using boxes describing regions of interrogation often enclose the vortex core as the closed path for evaluating the fluid circulation.<sup>7,12</sup> From the formulation, positive values signify counter-clockwise (CCW) rotation, whereas negative values represent clockwise (CW) motion of the fluid.

We perform statistical quantification of the flow properties to characterise the vorticity distribution. The histogram that is produced based on the percentage of map area versus the vorticity values  $\omega(s^{-1})$  throughout the entire flow map is featured in Figure 1(b). A high resolution of the histogram bins causes the histogram bar width to be overly small, and we propose the display of a frequency graph using a line that joins the height of each bar. In addition, we smooth the lines using spline interpolation to provide a more moderate estimation of the true frequency from each discrete bar height.

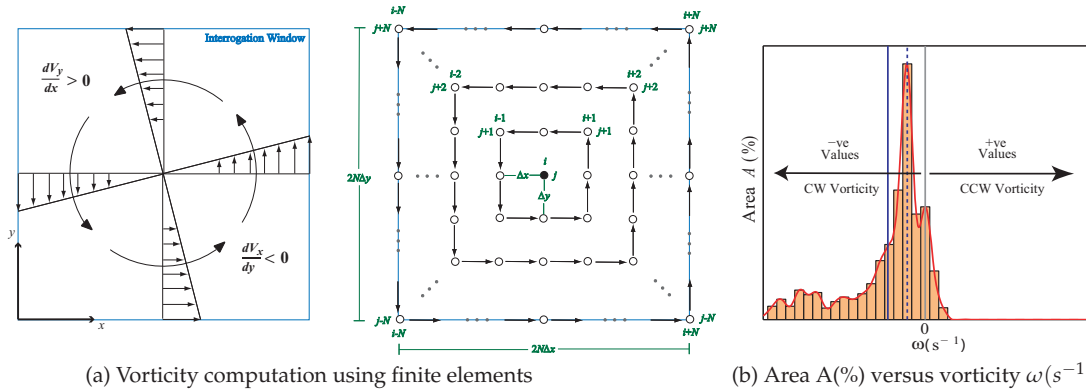


Figure 1: **Vorticity measurement and its histogram representation of the computed map.** Display of vorticity and calculations based on vectors along contour of flow around a node or usually a pixel in the flow vector image. Vorticity computation is based on the curl of vectors about a point of interest. Histogram depicting the variation of vorticity within the region of analysis gives an indication to the degree of rotation within the fluid. Flow investigations can be carried out by analyzing these histograms describing flow maps.

A quantification of average vorticity map value is computed by taking the mean,  $\bar{\omega}_\mu$ , or median,  $\bar{\omega}_m$  of the frequency histograms generated from vorticity maps. The magnitude of these parameters is represented as the blue solid and dash lines, while the centre zero  $\omega$  line is superimposed onto the frequency graph in grey. The vorticity standard deviations from the flow map measures the relative scatter around the mean and median of the vorticity values in the map respectively. Standard deviation  $\sigma$  with respect to  $\mu$  can be computed by considering the variation about the mean, and is denoted as  $\sigma_\mu$ . Based on a similar mode of computation, calculating the degree of variation about the median will give  $\sigma_m$ .

### 3. METHODS

Using mathematically generated velocity information based on the Oseen vortex, we have examined the flow with different vorticity. This allows us to simulate the principal features of a vortical flow in space. We assumed that the length scale corresponding to one standard deviation of the Gaussian vorticity distribution,  $L$  is 1 mm. The computational domain is  $(-5L \leq x \leq 5L)$  and  $(-5L \leq y \leq 5L)$ , which is equivalent to  $(-5 \leq x \leq 5)$  mm and  $(-5 \leq y \leq 5)$  mm, whereby  $(x, y)$  represents the Cartesian coordinates of the flow field, and the vortex has been scaled such that its maximum tangential velocity is  $10 \text{ mms}^{-1}$ . A digital image of 160 by 160 pixels represents the velocity flow field of this vortex.

We have discussed the concept to generate vorticity which is a means of measuring the angular rotation of fluid. Based on the measured velocity field, interrogation areas of some defined sizes are varied for the vorticity calculations, since the aim of our experiment is to test the modification of vorticity quantification based on changes in the vorticity sampling windows. Regions where the sampling windows are exposed partially outside the frame at the edge of the image will be padded with zero velocity vectors.

#### 4. RESULTS

In this study, we apply sampling mask sizes for vorticity computations ranging from  $(3 \times 3)$  to  $(67 \times 67)$  pixels or frames. Each frame has a dimension of  $\frac{1}{16}$  mm. Therefore we are looking at sampling frame sizes of  $(0.189 \times 0.189)$  to  $(4.19 \times 4.19)$  mm. Note that the vorticity map spans 10 mm by 10 mm. The analysis is performed for flow fields with 0%, 5%, 10%, 15%, 20% and 25% noise. As an illustration, we display the flow results for the set with 10% noise here.

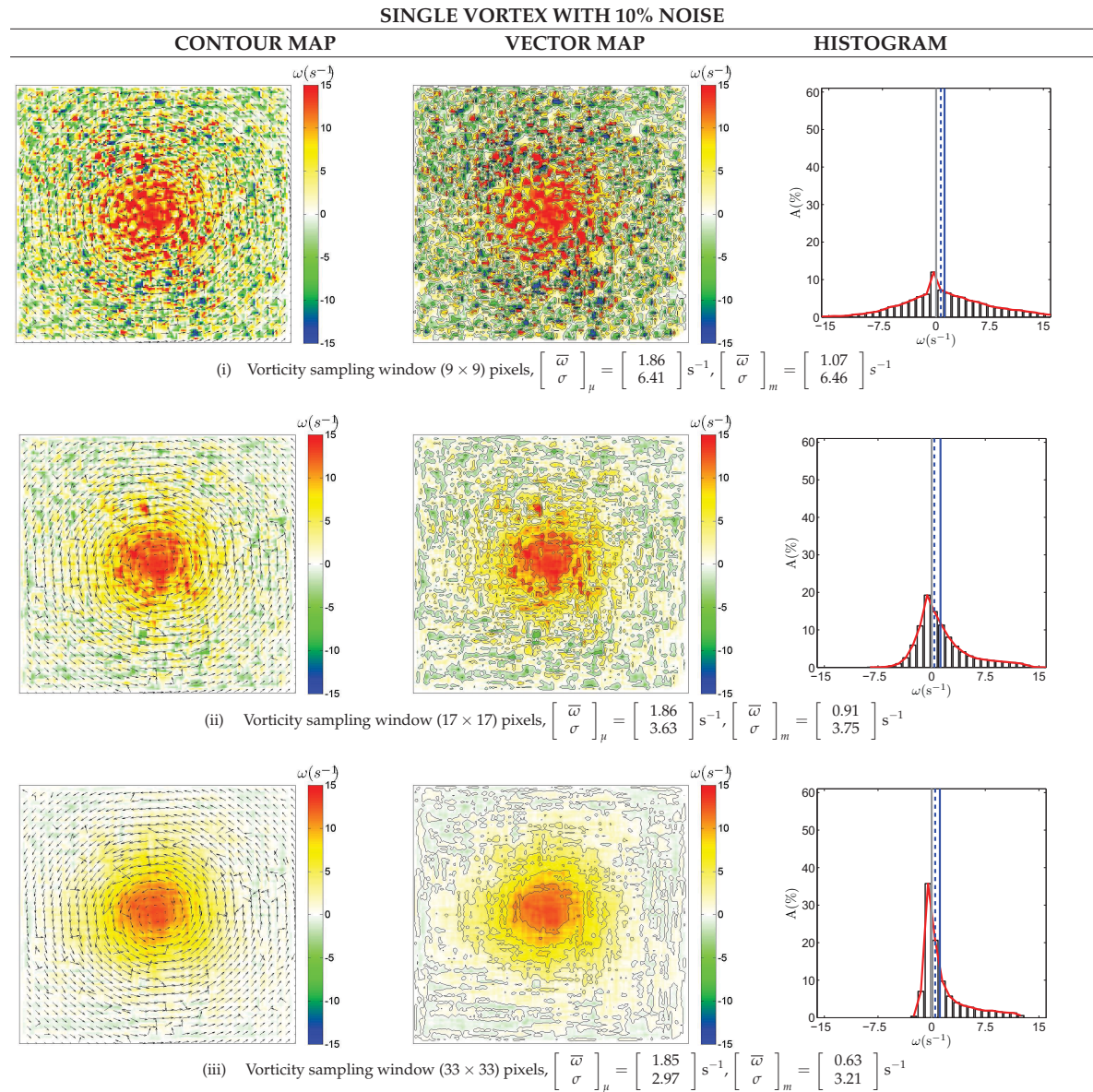


**Figure 2: Flow visualisation of Oseen vortex (10% noise).** Flow visualisation is performed on the Oseen vortex flow field with 10% noise added to it. The vorticity contour maps can produce an indication of the swirling of fluid with different degrees of smoothing relative to the sampling window size of the vorticity computation in the range of  $(9 \times 9)$  to  $(33 \times 33)$  pixels size or  $5.62 \times 10^{-2}$  to  $2.06 \times 10^{-1}$  times relative to the image of 160 by 160 pixels. Histograms pertaining to each and every of the vortex map are presented in the last column.

## 5. DISCUSSION

It is critical to establish a form of measure for reliability of the system to accurately develop vorticity maps of flow imaged by a given technique. The reliability of the vorticity measurement  $\rho$  can be defined as the ratio of the true vorticity variance to total variance that comprises the true and error components Bohrnstedt83,

$$\rho = \frac{\sigma_{\text{True}}^2}{\sigma_{\text{True}}^2 + \sigma_{\text{Error}}^2}, \quad (3)$$

where  $\sigma_{\text{True}}^2$  is the variance pertaining to the vorticity map of the ideal vortex, which is measured using a  $(3 \times 3)$  sampling window size, whereas that of the measured variance given by vortical flow field with noise is equivalent to  $\sigma_{\text{True}}^2 + \sigma_{\text{Error}}^2$ . To obtain the error map of a vorticity field measured based on a sampling window dimension, pixel by pixel differencing between the ideal vorticity image with that of the measured one based on a different vorticity configuration is conducted. The computation of the error variance in our measurement is based on the standard deviation of this error map. Reliability curves based on 5 to 25% noise are plotted as a function of sampling window sizes and shown in Figure 3. The sampling window size ratio is defined as the ratio of the window dimension in terms of pixels with respect to the vorticity image width.

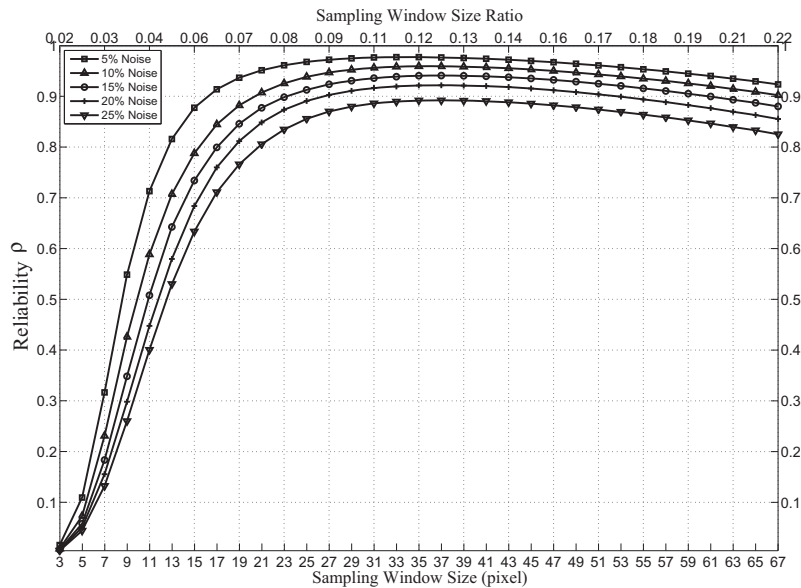


Figure 3: **Reliability test for single vortex flow fields.** Reliability for the flow field  $\rho$  calculated based on standard deviation  $\sigma_{\mu}$  of flow maps respectively. The variation of vorticity sampling window size can affect the reliability of computational measurement of the vorticity.

Note that the reliability of vorticity measurement improves for larger sampling window sizes. The optimal reliability occurs for a specific size and is dependent on the degree of noise added to the vector flow field. From the graphs, the optimal sampling window to use for vorticity maps based on a single vortical flow with 5, 10, 15, 20 and 25% noise is the  $(35 \times 35)$  pixels frame. This corresponds to a metric size ratio of 0.12 mm with respect to the image width of 160 pixels or 10 mm.

## 6. CONCLUSION

A statistical framework has been formulated to measure the strength of vortices in a fluid flow. The quantification of the vortices is based on the vorticity map of the imaged flow, and can give indications of the rate of

rotation as well as the number of vortices in a flow system under specified conditions. To validate this system, we have produced analytical flow field maps for testing vorticity measurements based on different configurations. The experiments show that the sampling window size of vorticity computation plays a role in defining the vortex accurately when there is noise in the flow measurement.

This paper has outlined the methodology used to obtain the vorticity or strain rates within the imaged fields in two dimensions. The primary objective of this study is to quantify characteristics of swirling fluid and therefore we have emphasised on the mathematical and computing aspects of describing flow vorticity and strains based on flow fields.

Furthermore, flow field sampling for vorticity calculation for different sampling sizes is carried out and results are statistically presented such that optimal vorticity measurement configuration can be selected. Using statistical analysis of the vorticity maps, we can deduce the criticality of the system reliability for the measurement of vorticity field. The procedures outlined in this study for assessing reliability can be used as a framework for determination of the optimised vorticity measurement configuration that is used for vorticity mapping that aid best in visualisation.

## REFERENCES

- [1] Alahyari, A. and Longmire, E., "Particle image velocimetry in a variable density flow: Application to a dynamically evolving microburst," *Experiments in Fluids* **17**, 434–440 (1994).
- [2] Raffel, M., Willert, C., and Kompenhans, J., [*Particle Image Velocimetry*], Springer-Verlag, Berlin Heidelberg, Germany (1998).
- [3] Raguin, L. G., Honecker, S. L., and Georgiadis, J. G., "MRI velocimetry in microchannel networks," *3rd IEEE/EMBS Special Topic Conference on Microtechnology in Medicine and Biology*, 319–322 (2005).
- [4] Cuzol, A., Hellier, P., and Mémin, E., "A low dimensional fluid motion estimator," *International Journal of Computer Vision* **75(3)**, 329–349 (2007).
- [5] Etebari, A. and Vlachos, P., "Improvements on the accuracy of derivative estimation from DPIV velocity measurements," *Experiments in Fluids* **39(6)**, 1040–1050 (2004).
- [6] Ferziger, J. H. and Peric, M., [*Computational Methods for Fluid Dynamics*], Springer (2001).
- [7] Fouras, A. and Soria, J., "Accuracy of out-of-plane vorticity measurements derived from in-plane velocity field data," *Experiments in Fluids* **25**, 409–430 (1998).
- [8] Hassan, E. R., Lau, T. C. W., and Kelso, R. M., "Accuracy of circulation estimation schemes applied to discretised velocity field data," *16th Australasian Fluid Mechanics Conference (AFMC)*, 142–145 (2007).
- [9] Saffman, P., [*Vortex Dynamics, 1st edition*], Cambridge University Press (1992).
- [10] Meunier, P., Dizes, S. L., and Leweke, T., "Physics of vortex merging," *Comptes Rendus Physique* **6(4-5)**, 431–450 (2005).
- [11] Cariteau, B. and Flór, J. B., "An experimental investigation on elliptical instability of a strongly asymmetric vortex pair in a stable density stratification," *Nonlinear Processes in Geophysics* **13(6)**, 641–649 (2006).
- [12] Weigand, A. and Gharib, M., "On the evolution of laminar vortex rings," *Experiments in Fluids* **22(6)**, 447–457 (1997).